*Desalination and Water Treatment*
www.deswater.com
doi: 10.1080/19443994.2015.1030703

57 (2016) 9115–9122
April

Taylor & Francis
Taylor & Francis Group

# Synthesis of titania–γ-alumina multilayer nanomembranes on performance-improved alumina supports for wastewater treatment

Masoud Shayesteh[a,*], Abdolreza Samimi[a], Mahdi Shafiee Afarani[b], Mohammad Khorram[a]

[a]*Faculty of Engineering, Department of Chemical Engineering, University of Sistan and Baluchestan, Zahedan, Iran, emails: shayeste@hamoon.usb.ac.ir (M. Shayesteh), a.samimi@eng.usb.ac.ir (A. Samimi), m_khorram@hamoon.usb.ac.ir (M. Khorram)*
[b]*Faculty of Engineering, Department of Materials Engineering, University of Sistan and Baluchestan, Zahedan, Iran, email: shafiee@eng.usb.ac.ir*

Received 29 July 2014; Accepted 9 March 2015

ABSTRACT

The γ-alumina and titania nanocrystallites were coated by sol–gel method on alumina supports respectively, as sub-layer and top-layer to prepare nanomembranes. The analysis represented a meso-porous structure for the coating layers of nanomembrane with the average pore size of 5.8 nm. The performance of the nanomembranes was investigated for permeability of demineralized water as well as rejection of ions and microorganisms using a model wastewater. Results show that in the range of 1–10 bar applied pressure, the permeability was reduced. At higher than 10 bars, with the increase of pressure, the permeability almost stayed constant due to the increase of flux. The multilayer nanomembranes showed different rejections for ions up to 25% but completely separation of the microorganisms.

*Keywords:* Nanofiltration; Nanomembrane; Slip casting; Rejection; Wastewater; γ-alumina; Titania

## 1. Introduction

It has reported that treatment of brackish and polluted water with nanofiltration (NF) normally produce a higher water flux and can often operate at lower pressures compared to RO, which reduces energy consumption [1]. Unlike RO, NF membranes can also perform better for the recycling of salt and reuse of many different wastewaters [2]. Nanomembranes are generally divided into two main groups: polymeric and inorganic ceramic. Clarifying further disadvantages of polymeric nanomembranes and benefits of ceramic nanomembranes during the past two decades drew the attentions toward the application of latter ones. In recent years, inorganic ceramic nanomembranes made of metal oxides such as alumina, zirconia, silica, and titania and non-oxides such as silicon carbide and silicon nitride have gained ground replacing the conventional polymeric nanomembranes [3,4].

Ceramic nanomembranes are generally fabricated as a monolayer and multilayered structure. The advantages of a monolayer membrane are its low cost and simple preparation procedure. However, monolayer membranes cannot perform NF processes. As a result, to have a membrane with high-performance parameters such as low cutoff values or high water

*Corresponding author.

fluxes, a multilayer configuration should be obtained [4,5]. Techniques such as slip casting, extrusion, or powder pressing have been so far used for manufacturing of support, followed by coating of several microns layers of different types of ceramics on it. For making of NF, one or more layers of coatings are necessary having pore size in the range of 1–50 nm to cover the support [6–10]. Among various methods of coating, chemical vapor deposition, sputtering [11], laser ablation, and sol–gel processing are used as preparation methods for thin films. In terms of sol–gel method, there are several coating techniques available such as slurry coating, dip coating, and spray coating [12,13]. The sol–gel process is recognized as low-temperature preparation leading to thin films of good homogeneity, high purity, and controlled chemical composition [14]. In fact, sols are primary state of colloids through which films are then produced through coating the support surface, followed by evaporating the solvent. The overall thickness of a ceramic membrane is therefore much higher (>2 mm), as compared to their polymeric counterpart. Nanocrystalline alumina and titania films have found applications in various areas, including UF and NF due to their resistances against different solvents, easy availability, high temperature withstanding capacity, and wider processing possibility [7].

This work reports the synthesis of titania–γ-alumina multilayer nanomembranes and the performance of the membranes. The results give some information concerning the rejection ratio of the membrane in acid and alkaline solutions. So, α-alumina tubes fabricated via slip casting route were used as the support for multilayered membrane. The intermediate γ-alumina sub-layer and titania as top-layer were coated sequentially on the support, and the water flux and permeability were characterized for the nanomembrane. The rejection of microorganisms and several ions was also determined for the nanomembrane using a model wastewater at different pH.

## 2. Materials and Methods

Alumina supports (external diameter = 47 mm, internal diameter = 43 mm, and height = 100 mm) with apparent density of 1.144 g $cm^{-3}$, volume porosity of 63.56%, and mean pore diameter of 0.25 μm were prepared according to a procedure reported elsewhere [14] using high-purity α-$Al_2O_3$ primary particles (WDR4, indal chemical, $d_{50}$ = 1 μm, BET surface area 1.5 $m^2$ $g^{-1}$, and purity of 99.4%) and $SiO_2$ powder (SYLOID AL-1 FP Pharmaceutical Excipient, $d_{50}$ = 6.8—8.1 μm, purity 99.4%) as starting materials. The sintering temperature was 1,420˚C for alumina green supports.

### 2.1. Preparing and coating of γ-alumina sub-layer on the support

Stable boehmite sol with the $d_{50}$ = 80 nm particle size was initially synthesized by hydrolyzing aluminum chloride hexa-hydrate ($AlCl_3{\cdot}6H_2O$, Merck), as precursor. Aluminum chloride solution was prepared by dissolving 12 g in 100 mL of water, and the pH of resulting solution was adjusted to 3. Ammonia solution was added slowly as a precipitating agent into the aluminum chloride solution under constant stirring until the pH of the precipitate reaches 9. The precipitate was filtered and washed with distilled water to remove the chlorides. The filtered powders prepared were dried in an electric oven at 80˚C for 24 h. The obtained wet cakes were poured in a beaker and diluted with distilled water to obtain boehmite suspension. A stable sol having pH of 3.5 was obtained by peptizing it by the addition of diluted nitric acid solution. The binder (PVA, MW = 72,000, Merck, 2 wt.% aqueous solution) was then added to boehmite sol (PVA: boehmite mass ratio of 0.85) to prevent cracking during drying [15,16]. The alumina supports were immersed in the sol for 5 s using a prototype programmable homemade dipping machine. The coated supports were placed at the room temperature for 24 h until the solvent evaporated and colloidal particles on the support surface shifted into gel-shape coat. The membranes were dried at 100˚C for 12 h, and then, they were heated to complete the calcination of boehmite and formation of γ-alumina layer at 550˚C for 3 h in an electric furnace under the heating rate of 5˚C $min^{-1}$.

### 2.2. Preparing and coating of titania top-layer on γ-alumina surface

For the synthesis of titania nanoparticles, tetra-n-butyl ortho-titanate (MW 340.36, Merck) was used as precursor and 2-propanol (2-PrOH) as solvent to reduce the concentration of alkoxide. Distilled water was dripped slowly until the white precipitate was formed. The precipitate was separated using a centrifuge and washed three times for removing of the alcohol. The sediment was then poured into a certain amount of distilled water while it was stirred at 50˚C for 2 h. Acid nitric (Merck, 0.1 M) was consequently used for peptizing the suspension to achieve pH 2. The obtained sol was kept at room temperature for

72 h, and a proper amount of PVA aqueous solution (2 wt.%) was then added to titania solution. Different dipping times were tested using the coating machine. However, 10 s dipping time was found suitable for our membranes that the intermediate layer of γ-alumina to be covered by the final layer of titania. After drying at room temperature and in the drier, the nanomembranes were heated at 350˚C for 3 h at the rate of 5˚C $min^{-1}$ to complete the calcination and formation of the titania layer.

### 2.3. Experimental setup and operation

The performance of the membranes was tested using a laboratory-scale reverse osmosis/ultrafiltration setup (Armfield FT18), while its tubular module was replaced with a module designed for our purpose. In Fig. 1, the flow diagram of the experimental NF installations and schematic design of the tubular module are shown. The ceramic membranes were inserted in the module, with a length of 100 mm and an OD of 47 mm.

During the experiments, the temperature was kept at 25˚C, while the collected permeate sample was recycled to the feed reservoir after measuring its volume. The applied pumping pressure was set in the range of 1–30 bar to keep the input flow rate to the module at 18 L $min^{-1}$. Distilled water was initially employed to characterize the flux and permeability of water through the nanomembranes, while a model wastewater was used to determine the rejection of ions and microorganisms. The model wastewater was made by mixing calcium sulfate, ammonium nitrate, and sodium chloride in distilled water. Then, municipal wastewater from the sewage tank was added to solution. The salt concentration of wastewater is listed in Table 1.

The final ion concentration in solution is listed in Table 2.

Table 2
Final concentrations of ions and total dissolved solids in sample water for filtering

| Component | $SO_4^{2-}$ | $Ca^{2+}$ | $NO_3^-$ | $Cl^-$ | TDS |
|---|---|---|---|---|---|
| Concentration (mg $L^{-1}$) | 94.5 | 68.6 | 103 | 212.4 | 530 |

### 2.4. Characterization of membrane properties and performance

Density and porosity of the supports were measured using Archimedes method, according to ASTM

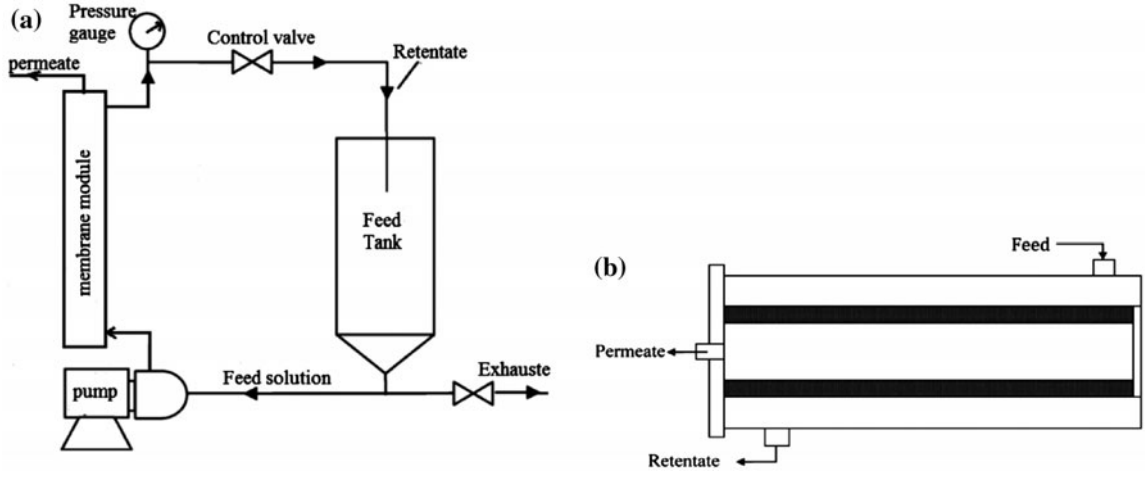


Fig. 1. (a) Flow diagram of ceramic membrane separation unit and (b) schematic drawing of tubular module employed for separation tests.

Table 1
The materials composition in sewage

| Materials | $MgSO_4$ | $FeCl_2$ | $KH_2PO_4$ | $K_2HPO_4$ | $MgCl_2$ | NaCl | KCl | $CaCl_2$ | $NH_4Cl$ |
|---|---|---|---|---|---|---|---|---|---|
| Concentration (g $L^{-1}$) | 0.007 | 0.03 | 6.2 | 4.2 | 6.3 | 0.6 | 0.66 | 0.3 | 0.03 |

C373-88. The simultaneous thermal analyzer (STA, PL-ATA-1640) was employed to study the thermal behavior of boehmite and hydrated titania. Microstructure analyses of samples were performed using field emission scanning electron microscopy (FE-SEM, MIRA\\TESCAN) and transmission electron microscopy (TEM, FEG PHILIPS CM200) techniques. XRD (Siemens, D-500, Germany) method was used for the structural characterization of samples. The particle sizes of boehmite and hydrated titania sols were determined using the dynamic laser beam scattering technique (SYMPATEC, NANOPHOX 0156 P). Nitrogen adsorption/desorption isotherms were obtained at 77 K to determine the pore size distribution of the multilayer nanomembrane (BEL Japan, Inc.).

## 3. Results and discussion

To determine the adequate temperature range for heat treatment of γ-alumina and titania layers, simultaneous thermal analysis of the dried gels was carried out in the air atmosphere. In Fig. 2 and Table 3, the STA curves and the temperature range in weight loss proceeds are presented. TGA curves illustrate that

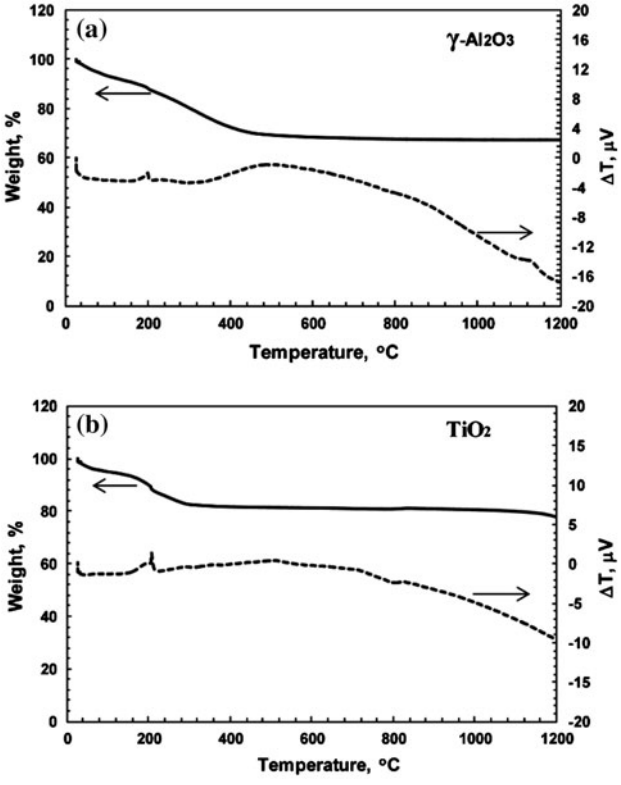


Fig. 2. STA curves for (a) boehmite and (b) hydrated titania.

Table 3
Different temperature ranges in weight loss proceeds

| | Substance | |
|---|---|---|
| Step | AlOOH (℃) | Titania.n$H_2O$ (℃) |
| Removing the water in porous gel network | 27–175 | 27–150 |
| Elimination of organic materials and nitric acid | 175−210 | 150–220 |
| Removal of residual structure water | 210–490 | 220–320 |
| Selected calcination temperature | 550 | 350 |

removal of residual structural water in boehmite occurs at higher temperature than hydrated titania. Furthermore, weight loss observed in boehmite is generally more than hydrated titania, representing higher calcination temperature for boehmite (550℃), as compared to hydrated titania (350℃).

Fig. 3(a) and (b) shows XRD patterns of obtained γ-AlOOH (card No. 10-0425) and titania (anatase card No. 84-1286) powders, respectively. Also, TEM micrographs of calcined sample at 550℃ (γ-alumina) and at 350℃ (titania) has been presented in Fig. 4.

The figure shows that the shape of nanopowder does not look precisely spherical. The size of nanopowder based on TEM analysis was smaller than 5 nm for both alumina and titania powders. Fig. 5(a) and (b) shows the average size and size distribution of boehmite and titania-hydrated sols, respectively. The average size of the particles in boehmite sol was found 80 nm and in titania-hydrated sol 20 nm with a narrow size distribution.

Fig. 6(a) and (b) shows cross section and surface of the membrane, respectively. It can be seen that the composite γ-alumina and titania layers compacted over the support with total thickness of about 7 μm (Fig. 6(a)). Moreover, a relative uniform surface layer was formed on the support as shown in Fig. 6(b).

For evaluating of the membrane performance, the volume of distilled water permeated through the membrane was measured at different transmembrane pressures for both the support and the nanomembrane. The permeate flux was calculated by dividing the collected permeate volume by the product of effective membrane area and the sampling time. Water permeability of the nanomembrane as a function of pressure in the range of 1–35 bars is compared with the support and shown in Fig. 7.

At it is seen, the permeability is initially (1–10 bar) decreased with the increase of pressure in the range of 30–15 L $h^{-1}$ $m^{-2}$ $bar^{-1}$ for nanomembrane. At the

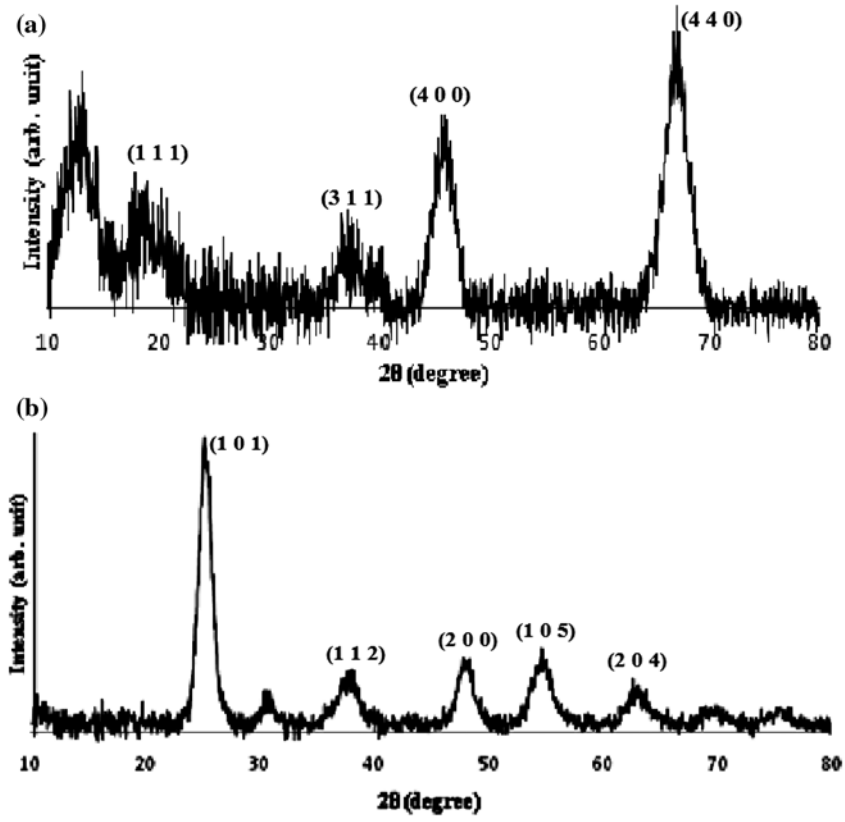


Fig. 3. XRD patterns of (a) γ-AlOOH and (b) anatase.

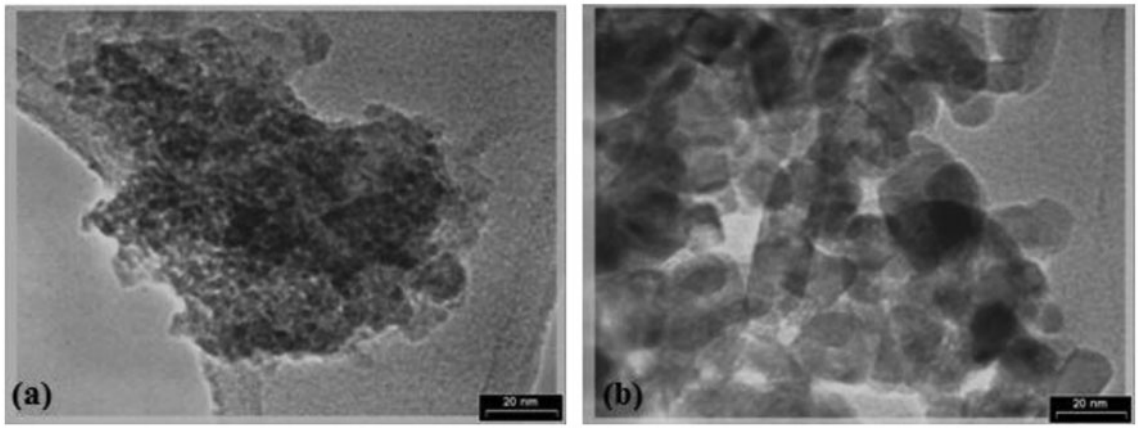


Fig. 4. TEM micrographs of agglomerated (a) γ-alumina powder and (b) titania powder.

pressures higher than 10 bars, the rate of permeability stayed almost constant at $12\ L\ h^{-1}\ m^{-2}\ bar^{-1}$ for nanomembrane. Such behavior was observed for supports as reported in our previous work [14]. In fact, at low pressures, the larger pores were being filled with water, and increasing the pressure did not enhance the flux, accordingly. At the higher pressures, as much as the pressure was increased, the water flux also increased in a same ratio. With rapid filling of small pores, the real permeability could be achieved at this stage [14]. Gas permeation mechanism can be changed from pure Knudsen flow regime to Poiseuille one with

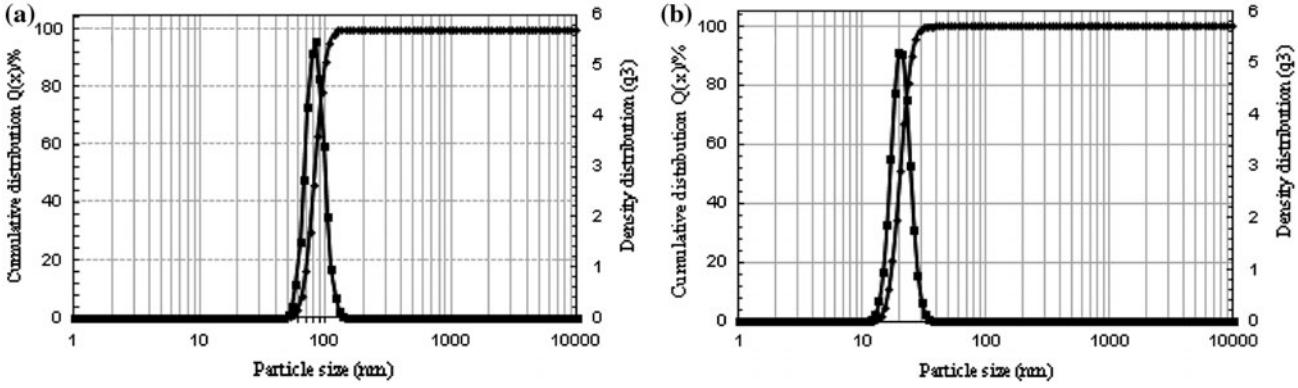


Fig. 5. The particle size distribution of (a) boehmite and (b) titania-hydrated sols.

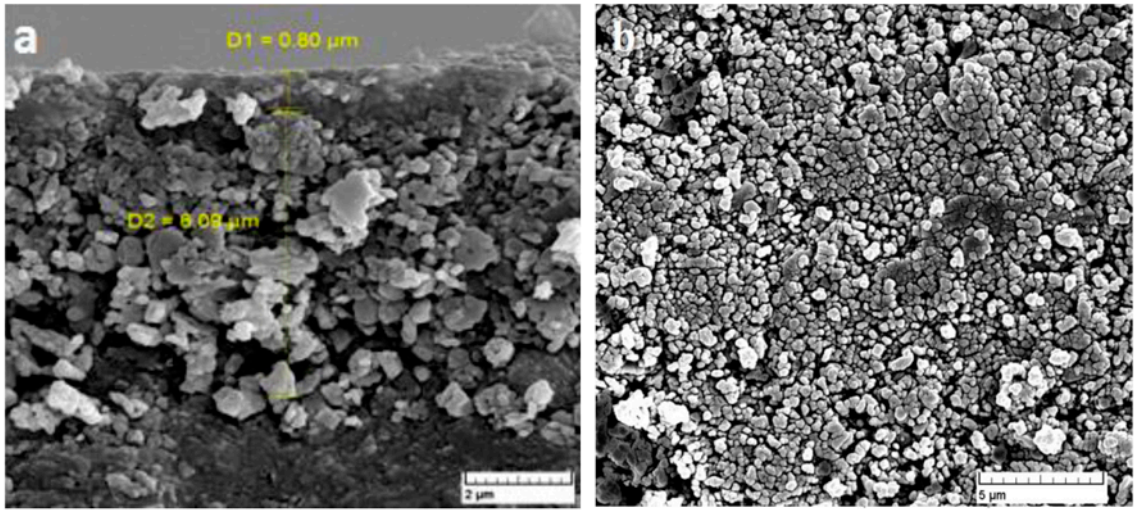


Fig. 6. SEM micrographs of alumina–titania composite membrane (a) cross-sectional view and (b) top-layer surface.

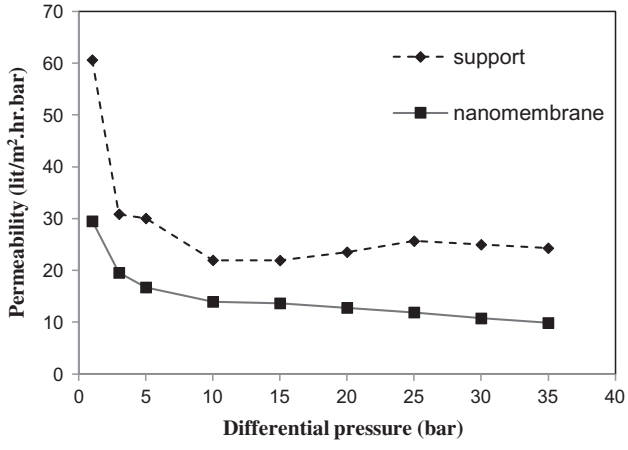


Fig. 7. Permeability of support and nanomembrane vs. differential pressure using distilled water.

pressure gas increase. Therefore, the trend observed in Fig. 7 is in opposite relation for gases, where the permeability vs. pressure is initially constant and then increases [17]. Comparing our results with the others shows that the permeate flux obtained for our nanomembrane is twice the flux reported in the work of Costa et al. at almost the same applied pressures [18].

Fig. 8 shows the rejection of some ions at pH 6.5 in different pressures for the nanomembrane.

Reduction of the rejection ratio of the most ions at pressures lesser than 10 bars is due to the high flux and subsequently changes in electrostatic forces on nanomembrane surface. Since the electrostatic attraction/repulsion force on the membrane surface can affect rejection ratio considerably, surface charge variation was performed with pH change. Therefore,

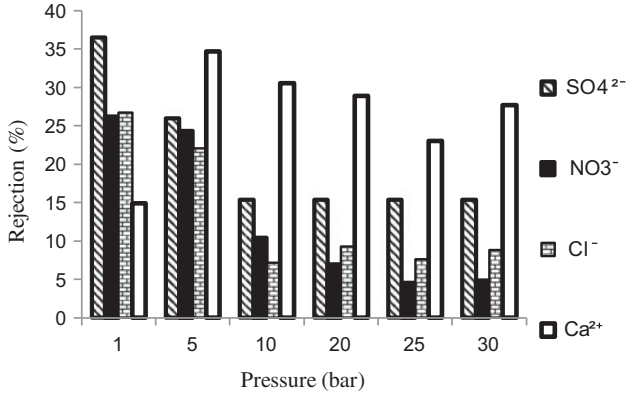


Fig. 8. Rejection ratio of some ions as a function of pressures for nanomembrane in pH 6.5.

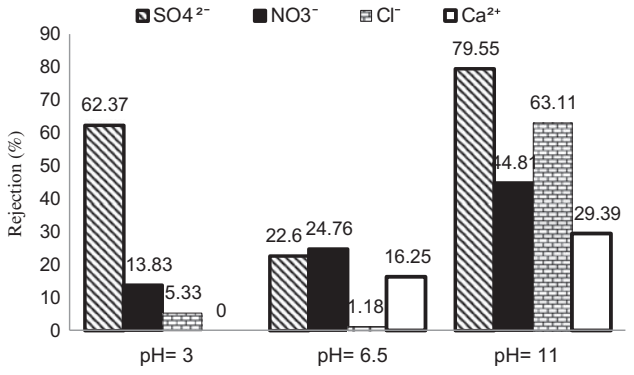


Fig. 9. Rejection ratio of four ions in acidic, normal, and alkaline pH for nanomembrane.

an acidic and an alkaline media were used for wastewater treatment. The rejection ratio of four ions is represented in Fig. 9.

Obviously, anions will have rejection ratio in alkaline pH than other pH range, but the larger size of the sulfate ion and its charge cause more rejection, while cations will have rejection ratio in acidic pH. However, calcium ions cause the inconsistency in our results. The reason for this difference could be the following: First, calcium ion radius is small compared with the radius of the other anions, and secondly, the sparingly soluble calcium sulfate has been used in the model solution. This salt is less ionized at high pH, and so, solid particles of calcium sulfate that are larger than the membrane pores do not pass through the membrane.

## 4. Conclusions

The tubular ceramic nanomembranes were fabricated using an evaluated support for the treatment of a model wastewater. The γ-alumina sub-layer and titania top-layer were prepared by calcination of dip-coated α-alumina supports in the colloidal boehmite and titania-hydrated sols, respectively. In the range 1–10 bar applied pressure, the permeability of water through the nanomembrane was decreased for nanomembranes. However, at the higher pressures, with increase of water flux, the permeability was almost constant. The rejection tests were conducted on a model wastewater containing the ions. The results showed that nanomembrane produced by support fabricated using slip casting method was able to reject partially the ions and could successfully separate all the microorganisms. The proper adjustment of pH can be increase the ion rejection.

## References

[1] J.M. Skluzacek, M.I. Tejedor, M.A. Anderson, NaCl rejection by an inorganic nanofiltration membrane in relation to its central pore potential, J. Membr. Sci. 289 (2007) 32–39.
[2] S.K. Nataraj, K.M. Hosamani, T.M. Aminabhavi, Nanofiltration and reverse osmosis thin film composite membrane module for the removal of dye and salts from the simulated mixtures, Desalination 249 (2009) 12–17.
[3] K.K. Chan, A.N. Brownstein, Ceramic membranes—Growth prospects and opportunities, Am. Ceram. Soc. Bull. 70 (1991) 703–707.
[4] T. Van Gestel, C. Vandecasteele, A. Buekenhoudt, C. Dotremont, J. Luyten, R. Leysen, B. Van der Bruggen, G. Maes, Alumina and titania multilayer membranes for nanofiltration: Preparation, characterization and chemical stability, J. Membr. Sci. 207 (2002) 73–89.
[5] A. Alem, H. Sarpoolaky, M. Keshmiri, Sol–gel preparation of titania multilayer membrane for photocatalytic applications, Ceram. Int. 35 (2009) 1837–1843.
[6] K. Keizer, A.J. Burggraaf, Porous ceramics material in membrane application, in: D. Taylor (Ed.), Science of Ceramics, fourteenth ed., The Institute of Ceramics, Shelton, 1988, pp. 83–93.
[7] A.F.M. Leenaars, K. Keizer, A.J. Burggraaf, The preparation and characterization of alumina membranes with ultra-fine pores, J. Mater. Sci. 19 (1984) 1077–1088.
[8] A. Larbot, J.A. Alary, C. Guizard, L. Cot, J. Gillot, New inorganic ultrafiltration membranes: Preparation and characterisation, Int. J. High Tech. Ceram. 3 (1987) 143–151.
[9] A. Larbot, J.A. Alary, J.P. Fabre, C. Guizard, L. Cot, Microporous layer from sol–gel techniques, in: C.J. Brinker, D.E. Clark, D.R. Ulrich (Eds.), MRS Proceedings, vol. 73, The Material Research Society, Pittsburgh, PA, 1986, pp. 659–664.
[10] M. Jiang, X. Liu, H. Wang, Conductive and transparent bi-doped ZnO thin films prepared by rf magnetron sputtering, Surf. Coat. Technol. 203 (2009) 3750–3753.
[11] A.F.M. Leenaars, A.J. Burggraaf, The preparation and characterization of alumina membranes with ultrafine pores. 2: The formation of supported membranes, J. Colloid Interface Sci. 105 (1985) 27–40.

[12] M. Morozova, P. Kluson, J. Krysa, M. Vesely, P. Dzik, O. Solcova, Electrochemical properties of $TiO_2$ electrode prepared by various methods, Procedia Eng. 42 (2012) 573–580.
[13] H. Choi, E. Stathatos, D.D. Dionysiou, Sol–gel preparation of mesoporous photocatalytic $TiO_2$ films and $TiO_2/Al_2O_3$ composite membranes for environmental applications, Appl. Catal., B, 63 (2006) 60–67.
[14] N.D. Heydarian, M. Shayesteh, M. Shafiee Afarani, A. Samimi, Effect of ammonium nitrate on microstructure and permeability of alumina support using slip casting fabrication method, J. Ceram. Process. Res. 14 (2013) 472–475.
[15] C. Falamaki, J. Veysizadeh, Comparative study of different routes of particulate processing on the characteristics of alumina functionally graded microfilter/membrane supports, J. Membr. Sci. 280 (2006) 899–910.
[16] H. Firouzghalb, C. Falamaki, Fabrication of asymmetric alumina membranes, Mater. Sci. Eng., B 166 (2010) 163–169.
[17] C. Falamaki, M. Naimi, A. Aghaie, Dip-coating technique for the manufacture of alumina microfilters using PVA and Na- CMC as binders: A comparative study, J. Eur. Ceram. Soc. 26 (2006) 949–956.
[18] A.R. Costa, M. de Pinho, Performance and cost estimation of nanofiltration for surface water treatment in drinking water production, Desalination 196 (2006) 55–65.